Ocean Systems Engineering, *Vol. 13, No. 3 (2023) 269-286*
https://doi.org/10.12989/ose.2023.13.3.269

CFD estimation of HDCs for varying bodies of revolution of underwater gliders

R.V. Shashank Shankar and R. Vijayakumar*

Department of Ocean Engineering, IIT Madras, Guindy, Chennai 600036, India

(Received January 26, 2022, Revised August 17, 2023, Accepted August 22, 2023)

Abstract. Autonomous Underwater Gliders (AUGs) are a type of Underwater Vehicles that move without the help of a standard propeller. Gliders use buoyancy engines to vary their weight or buoyancy and traverse with the help of the Lift and Drag forces developed from the fuselage and the wings. The Lift and Drag Coefficients, also called Hydrodynamic coefficients (HDCs) play a major role in glider dynamics. This paper examines the effect of the different types of glider fuselages based on the bodies of revolution (BOR) of NACA sections. The HDCs of the glider fuselages are numerically estimated at a low-speed regime (10^5 Reynolds Number) using Computational Fluid Dynamics (CFD). The methodology is validated using published literature, and the results of CFD are discussed for possible application in the estimation of glider turning motion.

Keywords: CFD; fuselage; glider; hull form; STAR CCM+

1. Introduction

Autonomous Underwater Gliders (AUG) are a class of Autonomous Underwater Vehicles (AUVs) that operate without a conventional propeller. They employ a change in buoyancy and hydrodynamic forces developed by the wings to move in a longitudinal up and down motion (called a sawtooth motion) and a turning motion (called spiral / helical maneuver). These maneuvers are shown in Fig. 1. AUVs possess propulsion mechanisms like thrusters that help the vehicle navigate efficiently (Saunders and Nahon 2002). However, these systems have higher power requirements. This makes the vehicle dependent on the battery characteristics for endurance. Gliders have higher endurance and range as the power requirements is lesser compared to typical AUVs.

The turning motion of gliders is of interest as the vehicle cannot execute an in-plane turn and the resulting trajectory is a spiral. The turning motion can be initiated using an external control surface like a rudder, internal rotatable mass or by variation of the angle of attack of wings as studied by Zhang *et al*. (2013) and Wang *et al*. (2017). The spiral path can be characterised by parameters that describe the speed and attitude of the glider during the turn. They can be estimated using a suitable dynamic model proposed by Zhang *et al*. (2014), and Shankar *et al*. (2019). The dynamic model is developed based on the forces on the glider that are acting on the glider during its motion as brought out in Fig. 2.

∗Corresponding author, Mr., E-mail: oe16d201@smail.iitm.ac.in

http://www.techno-press.org/?journal=ose&subpage=7 ISSN: 2093-6702 (Print), 2093-677X (Online)

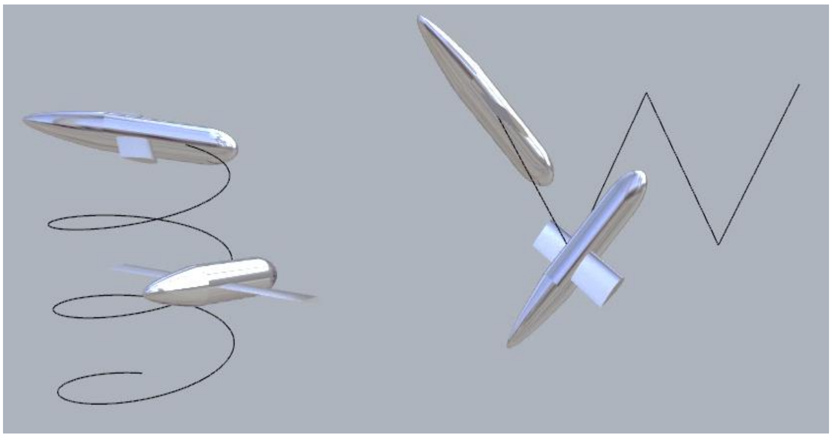

Fig. 1 Glider characteristic maneuver. Turning path in the left and “Sawtooth” motion on right

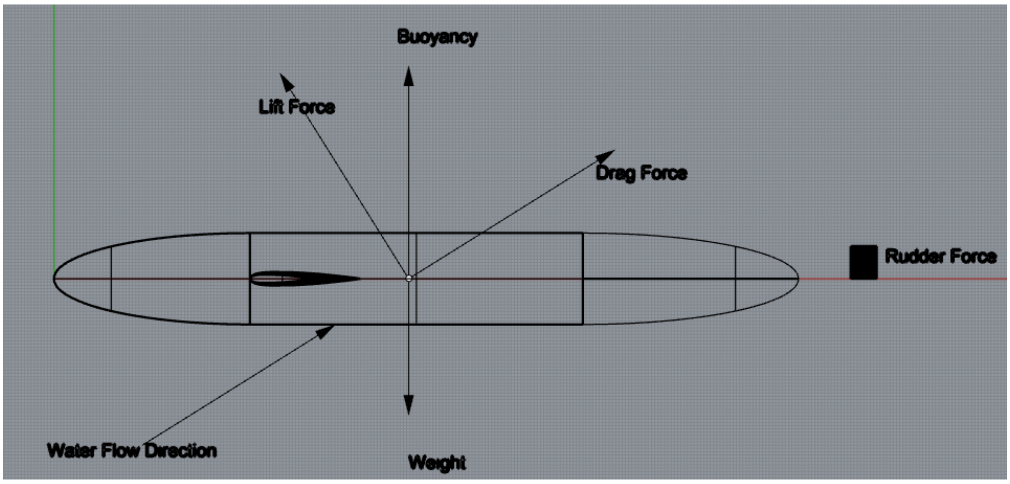

Fig. 2 Forces on the Underwater Glider

The hydrodynamic coefficients of the underwater gliders are influenced by the geometric parameters of the gliders such as wings, fuselage, and rudder. The study of wings and wing form of the gliders have been undertaken previously by many researchers namely, Yasar *et al.* (2015), Hockley (2018), Shankar *et al.* (2020), Sun *et al.* (2021). However, research on the fuselage of AUG is limited. Ting et al., (2012) showed that the fuselage accounts for more than 20% of the lift force and 45% of the drag force developed by a glider. The hull form of a glider also acts as a shroud for encompassing the pressure-proof hull of the glider. A previous review undertaken by the authors of this paper (Shashank and Vijayakumar 2019), discussed the importance of the spiral path and its characteristics. One of the conclusions of the study was the gap in the literature regarding the effect of hull form on the turning trajectory of gliders.

This article evaluates the effect of change in hull form on the hydrodynamic coefficients. The study is undertaken by evaluating the lift and drag coefficients of four gliders and analysing how the variation of the fuselage, keeping the volume constant, affects the hydrodynamic characteristics thereby influencing the maneuverability of the vehicle.

2. Studies on hull forms of underwater bodies

The hull form of underwater gliders can be classified into two types: -

(a) Torpedo shaped "Legacy Gliders" like Slocum, Spray.

(b) "Blended wing Body" (BWB) gliders like Liberdade.

The Blended Wing Body gliders, due to their high Lift/Drag ratio (compared to legacy gliders) are employed for faster longitudinal motion and find usage in military applications as discussed by Ray *et al*. (2011). Their performance and shaping have been extensively explored by various authors (Guggilla and Rajagopalan 2018, 2019, 2020, Guggilla and Vijayakumar 2019b, Li *et al*. 2020).

This study is focused on torpedo-shaped conventional or legacy underwater gliders. The hydrodynamic design of AUGs is associated with the literature of aeroplanes and submarines. The study of streamline sections for usage as vehicle forms in the study of aerodynamics and hydrodynamics has been undertaken by various researchers. Hoerner (1965)presented the results of Drag as a function of Reynolds Number for various families of sections which included sections used for struts, fuselage, nacelles etc. Further, a large number of experimental and numerical studies exist for flow past bodies of revolution (Li *et al*. 2020, Krasnov 1971, Joubert *et al*. 1978, Heaslet and Nitzberg 1947).

Literature on submarines describes the hull as a combination of the entrance, run and parallel middle body. The Length to Diameter (L/D) ratio of 6-8 is considered ideal for submarines with drag reduction as the criteria. The forward section of a submarine is evaluated by three desirable criteria, as discussed by Jackson (1992):-

(a) smallest negative pressure coefficient

(b) smallest pressure gradient

(c) minimum value of the pressure coefficient as far aft as possible

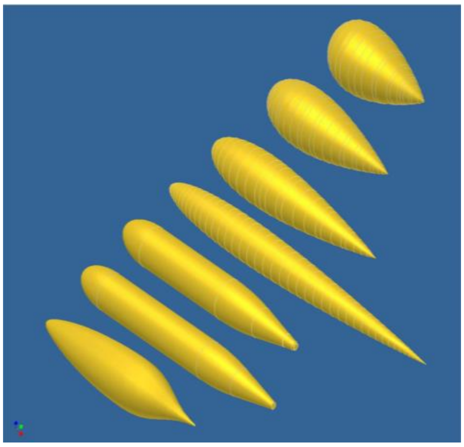

Fig. 3 Standard AUV Bodies. left to right Laminar Flow Body, Autosub l to 3, Autosub 6000, NACA 0010, NACA 0020, NACA 0033, NACA 0050 (Stevenson *et al*. 2007)

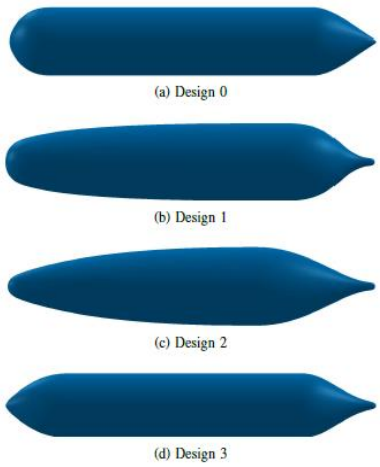

Fig. 4 Hull forms for AUGs evaluated for drag performance (Lidtke *et al*. 2016)

The shape of the stern of a submarine is designed in conjunction with the propeller. Propulsive efficiency is the criteria for such a design. The literature on hull forms of AUVs also finds application in the study of gliders.

The different types of hull forms of AUVs were classified by Stevenson *et al.* (2007) as:-

(a) Conventional torpedo proportions, large and small.

(b) Laminar flow, bulbous hull to reduce drag.

(c) Streamlined rectangular style.

(d) Multihull vehicles splitting the energy, propulsion and mission management from the sensor payload into separate hulls.

Fig. 3 shows these different types of hull forms. Further, the authors studied the Laminar shape, Autosub (Torpedo Shape) and National Advisory Committee for Aeronautics (NACA) profiles. They suggested that the drag behaviour of Laminar shaped bodies is more efficient than the torpedo form, with the requirement that all ancillary protrusions are kept in the rear of the body. Stevenson *et al.* (2007) also indicated that the practicalities of populating the NACA body of revolution hull forms and handling issues are easier with a stubby design. The range of Reynolds numbers (with length of the vehicle used as characteristic dimension) for which the analysis was undertaken was greater than 10^6. This is on the higher side of velocities of legacy underwater gliders which operate at a lower speed of 1-2 knots (compared to AUV speed), which translates to Reynolds number of order of 10^5 for gliders.

Lidtke *et al*. (2018) discussed the process of designing an appropriate hydrodynamic shape for a hybrid underwater glider with the design having intermediate stages including axisymmetric hull shape, hydrofoils, and appendages. The hull forms studied were variations of Laminar flow body shapes, and the images of the hull forms are indicated in Fig. 4. The study indicated Natural Laminar Flow (NLF) hull form for better drag performance.

The observations and limitations of the studies on underwater hull forms is as follows:-

(a) Drag values for various sections, while existing, do not include information about the variation with the angle of attack of the flow at the transition Reynolds number range (10^5).

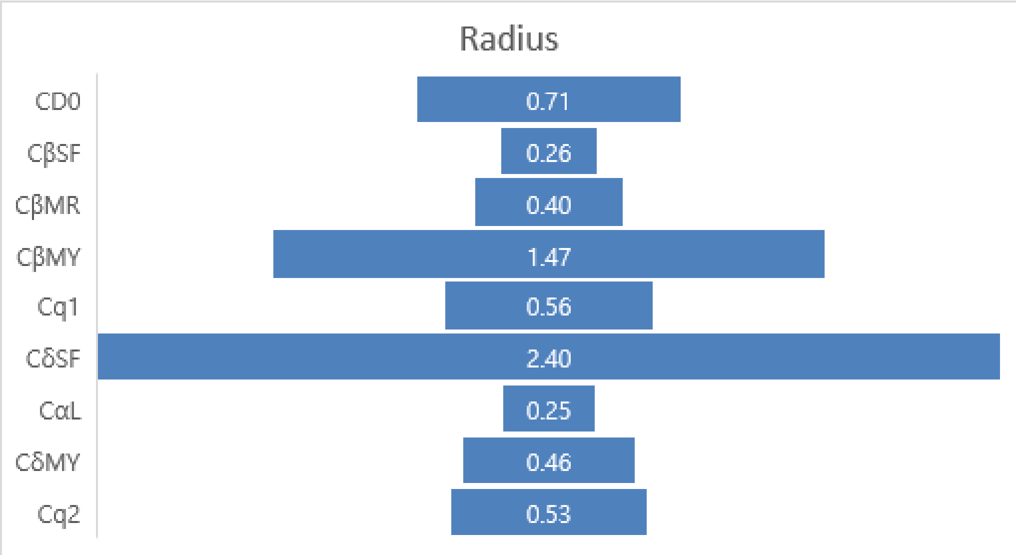

Fig. 5 Sensitivity of the Radius of the Spiral path on the viscous HDCs (Rayaprolu and Vijayakumar 2021)

(b) Study of drag of streamline sections, along with standard wings for the Reynolds number of operation of gliders is not extensively found.

(c) The pressure coefficient and the distribution of pressure at the flow Reynolds number is necessary for the comparison of hull forms.

(d) The aft body design and the criteria for the stern shape for a glider is a gap area.

(e) For an AUG with a turn initiated by roll control mass, the Lift forces generated play a dominant role (as the centripetal force) in the turning motion. The radius of the spiral path is inversely proportional to the lift produced and hence the maneuverability of the glider is dependent on the lift coefficients of the glider.

(f) Similarly, for an AUG with a turn initiated by a rudder, the drag of the glider plays a dominant role in maneuverability.

(g) A sensitivity analysis of the turning motion of the underwater gliders carried out by the current authors identified the important hydrodynamic coefficients that affect the turning motion characteristics of a glider (Rayaprolu and Vijayakumar 2021). The sensitivity plots for the radius of the turning motion initiated by the rudder is brought out in Figure 5 where, the sensitivity of the radius of the glider's turning motion to each of the hydrodynamic coefficients of the underwater glider is shown. The sensitivity indicated depicts the change in the radius of the glider against the change in HDC. For example, a change of ε% in C_{D0} will lead to a change in 0.705 times ε% in the radius of the glider's turning path.

A comparison of a constant volume study on the body of revolutions with emphasis on Lift and Drag characteristics is expected to aid the study of glider maneuverability. The hull form sections mentioned above (NACA 0010, NACA 0020, NACA 0033) in particular can be studied with emphasis on the Lift and Drag characteristics at the angles of attack experienced while a glider is executing a turn. The methodology involves selecting a baseline candidate glider hull and then varying the shape of the body while keeping the volume constant. While such a study may not be considered “parametric” in a true sense, it will provide reference data for designers who are exploring the shapes of hull forms for gliders to suit the payload.

The lift and drag characteristics across various angles of attack studied can be analysed by curve fitting techniques for extracting hydrodynamic coefficients of gliders that can be used for trajectory estimation (Singh *et al.* 2017), (Stryczniewicz *et al*. 2019). The curve fitting involves plotting of RMS Drag coefficient values and mean Lift coefficient values against the angle of attack (in degrees).

The resultant trendline coefficients can be used to study the lift and drag force of a glider. The relevant equations are as shown below (Mises 1945)

$$C_D = C_{D0} + C_D^{\alpha}\ \alpha^2 \tag{1}$$

$$C_L = C_{L0} + C_L^{\alpha}\alpha \tag{2}$$

Wherein, the terms of the equation are defined as follows:-

C_D= Drag coefficient

C_L= Lift coefficient

α = Angle of attack

C_{D0}=Drag at 0˚ Angle of attack

C_{L0}=Lift at 0˚ Angle of attack

C_D^{α}=Coefficient of the second order variable for the curve of drag coefficient plotted against angle of attack

C_L^{α}= Coefficient of the first order variable for the curve of lift coefficient plotted against angle of attack

3. CFD Study on underwater glider hull form

The methodology adopted for the analysis is as follows: -

(a) Lift and drag forces developed on the glider “Alex” are estimated using CFD and compared with published results of Arima *et al*. (2008) for the validation of the CFD methodology. The methodology thus validated will be used for assessing glider fuselage characteristics.

(b) The hull form of a baseline glider developed is varied by keeping the volume same (with the variation of volume kept less than 2%). The performance of all the three variants w.r.t to the baseline glider are compared.

3.1 Validation of CFD methodology

The ALEX glider developed by Arima *et al*. (2008) and was analysed using CFD for validation of methodology. The analysis was undertaken using commercially available CFD solver STAR-CCM+, a copyrighted software. The Alex glider is a legacy shaped underwater glider. The length of the Alex glider is 0.83 m and the diameter is 0.085 m. SST Menter K-ω turbulence model has been used based on work done by Jagadeesh *et al.* (2016). A grid independence study was undertaken with surface re-mesher, prism layers and polyhedral meshing models in STAR-CCM+. The minimum number of cells after which the values do not change was found to be of the order of 10^6 cells. The study is undertaken to assess the C_L and C_D of the glider with the change in Angle of Attack (α).

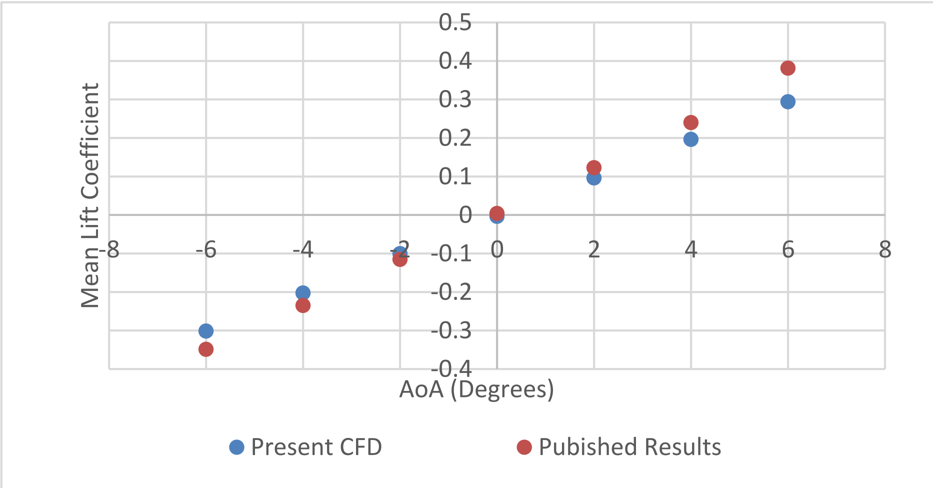

Fig. 6 Mean Lift Coefficient Results for Validation (Published results refer to the experimental results of Arima *et al*. (2008))

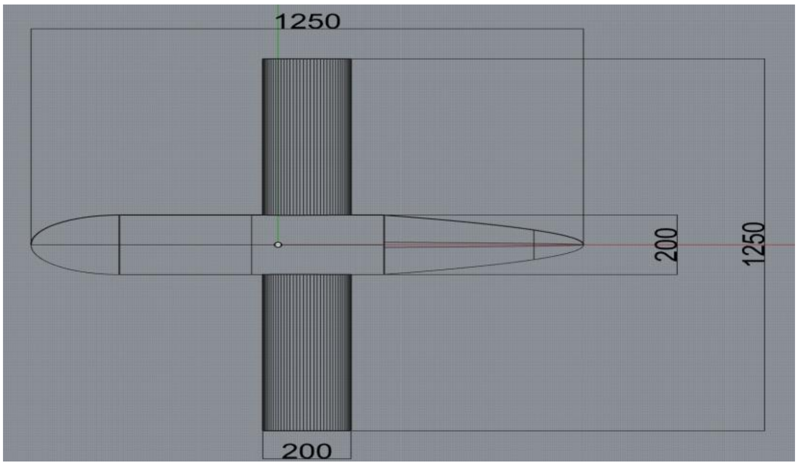

Fig. 7 Candidate baseline underwater glider CAD model. The dimensions of the glider are shown in mm

The values of Lift coefficients obtained using CFD are compared with experimental values of published literature (Arima *et al*. 2008). The mean Lift coefficients obtained for angles of attack from -6˚ to +6˚ are plotted for the current CFD study and compared with the published results in Fig. 6. The error percentage for the Lift coefficient is found to be 17%.

Then, a candidate glider was modelled in CAD software (Fig. 7), and three glider hull forms were developed (Fig. 8). The candidate glider geometry is similar to a legacy glider with the hull form shaped in a torpedo shape and wing located symmetrically. The dimensions of the glider geometry

Table 1 Geometric parameters of baseline glider and variants

Model	Length (m)	Span (m)	Diameter of Fuselage (m)	Surface Area (m^2)	Volume (m^3)	% Difference in Volume w.r.t Baseline Glider
Baseline Glider	1.250	1.250	0.2	1.105	0.0336	NA
NACA 0010	1.875	1.228	0.189	1.212	0.0334	-0.272%
NACA 0020	1.186	1.269	0.242	1.064	0.0340	1.38%
NACA 0033	0.796	1.297	0.285	0.967	0.0336	0.278%

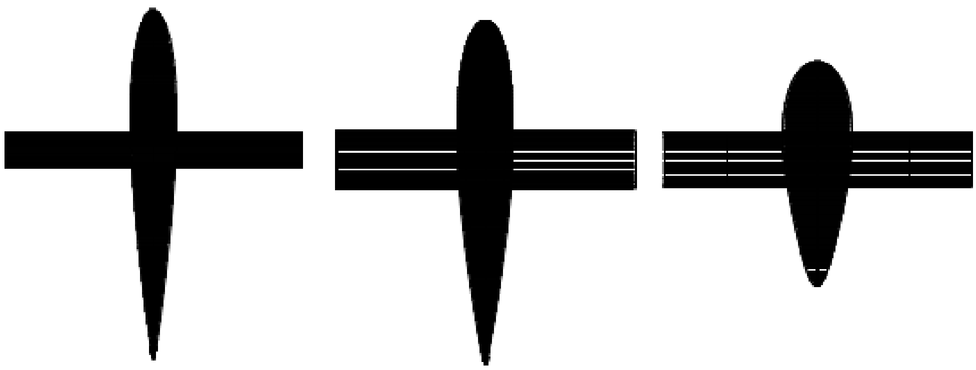

Fig. 8 Body of Revolution generated considering 2D sections of NACA0010, NACA0020 and NACA0033 (Left to Right)

are shown in Fig. 7 (in mm). Further description of the geometry is detailed in the next section. The volume of all three models is nearly equal to that of the baseline glider (volume variation less than 1.5%). Investigation of C_L and C_D on these models with a change in the angle of attack (range -6˚ to +6˚) for five velocities (range 0.1 to 0.5 m/s) was undertaken.

3.2 Study of hull form variation

The variation of hull form is undertaken by keeping the total volume of the glider (body and wings) as a constant and obtain a variant with the fuselage of NACA section revolved and wing of NACA0012 section of chord length 0.2 m. The baseline fuselage is developed as per Guggilla *et al*. (2019a). The nose section is an ellipsoid with a minor axis length of 0.1 m and a major axis of 0.2 m. The cylindrical parallel middle body is of length 0.6 m with a 0.2 m outer diameter. The paraboloid aft section is of length 0.45 m making the fuselage length of 1.25 m. The wingspan is selected to equal the fuselage length and the chord length is taken equal to the diameter of the fuselage. The wetted surface area of the glider is 1.105 m^2 and the volume of the glider is 0.0336 m^3. The details of glider geometric parameters for all four gliders are brought out in Table 1. The difference in volume amongst the variants is less than 2%.

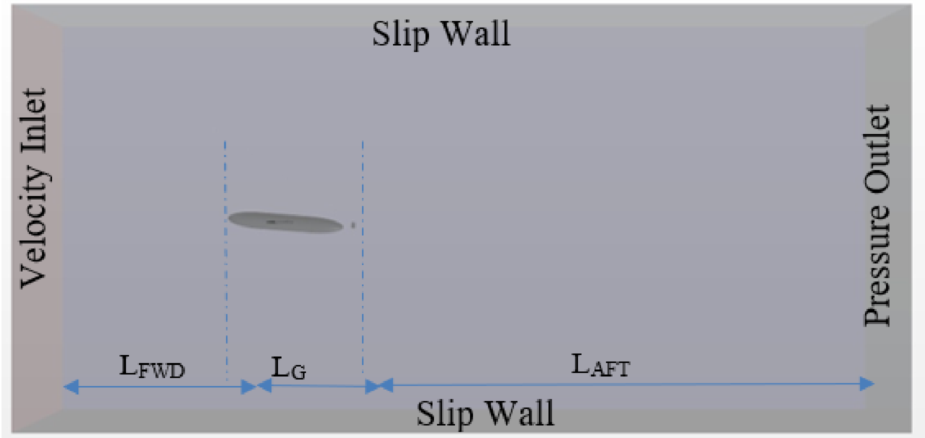

Fig. 9 Domain for CFD Studies

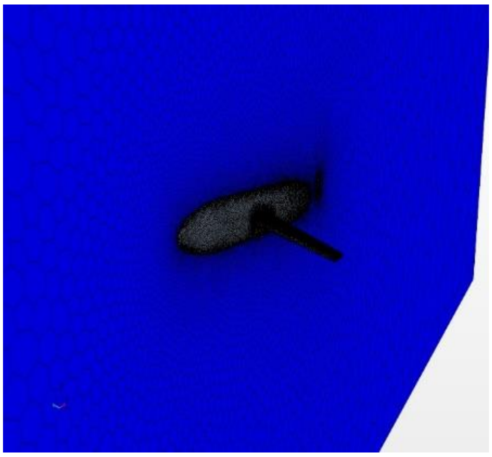

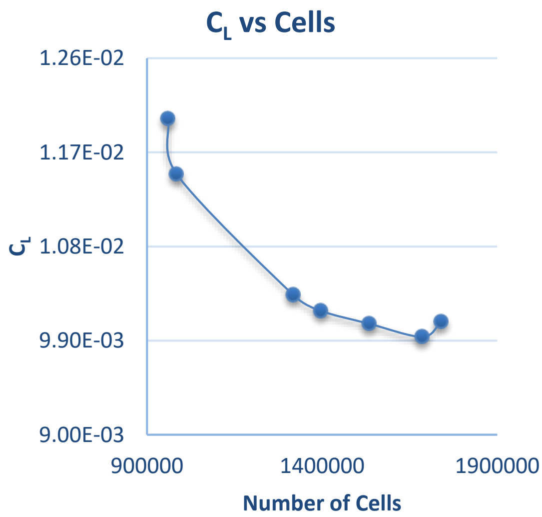

(a) Half Domain and mesh of the glider

(b) Grid independence study results

Fig. 10 Domain Studies

3.3 CFD domain

The domain dimensions used for the study are taken as per ITTC recommendations for Marine CFD applications (ITTC - Recommended Procedures and Guidelines 2011) and shown in Fig. 9. L_G is the Length of the Glider, L_{FWD} is $1.3L_G$, and L_{AFT} is $5L_G$. The sidewall domain distance is also taken as $1.3L_G$. Boundary conditions are also shown in Fig. 9. A 3D, steady flow condition was chosen for the CFD study. The mesh size was reduced by meshing only one half of the domain and

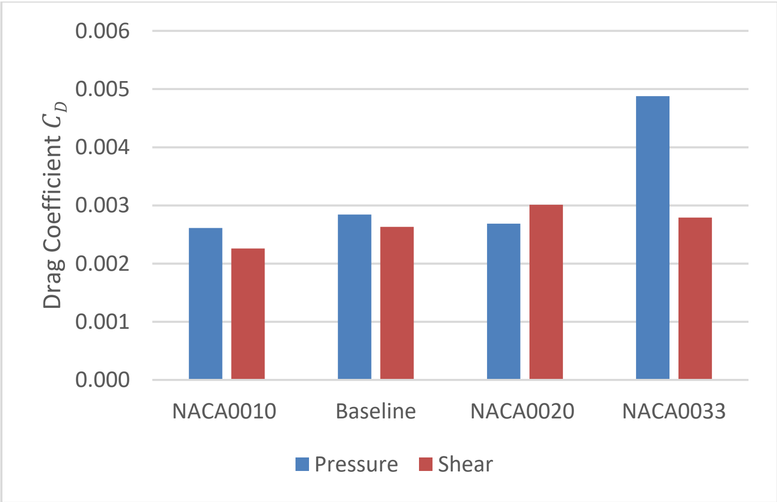

Fig. 11 Comparison of Drag Force Coefficient (C_D) for all the four gliders

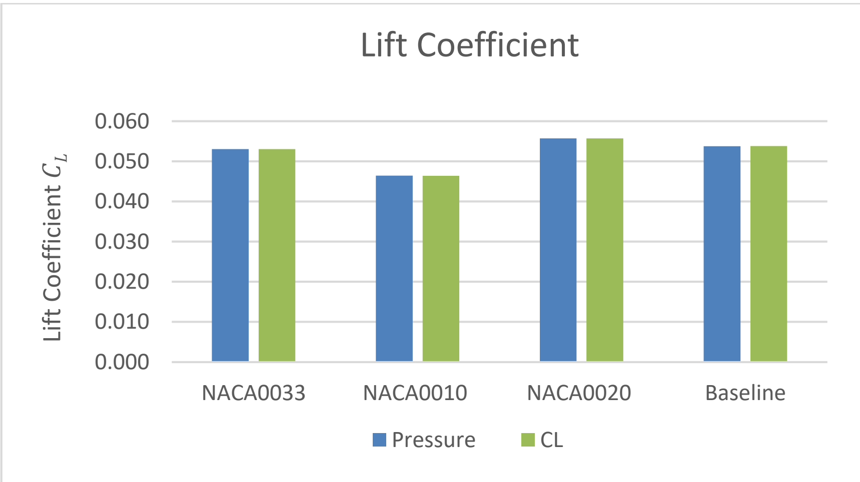

Fig. 12 Comparison of Lift Force Coefficient (C_L) for all the four gliders

assigning symmetry boundary conditions to the middle plane (Fig. 10). This was undertaken as the body was axisymmetric, and the study involved a change in the angle of attack alone. A grid independence study was undertaken, and the results are also placed in Fig. 10. The number of cells was found to be 3.4 million. The meshing models used involve polyhedral meshes with prism layers calculated as five layers with a stretching factor of 1.5. The total boundary layer thickness was calculated to be 0.021 m. The Reynolds number of the flow varies from 10^5 to 10^6. SST (Menter) K-ω turbulence model was chosen with a grid point for the first cell at y+<1. This model was found to predict flow characteristics near the wall with better accuracy compared to other models as per literature as shown by Singh *et al*. (2017), and Li *et al*. (2014).

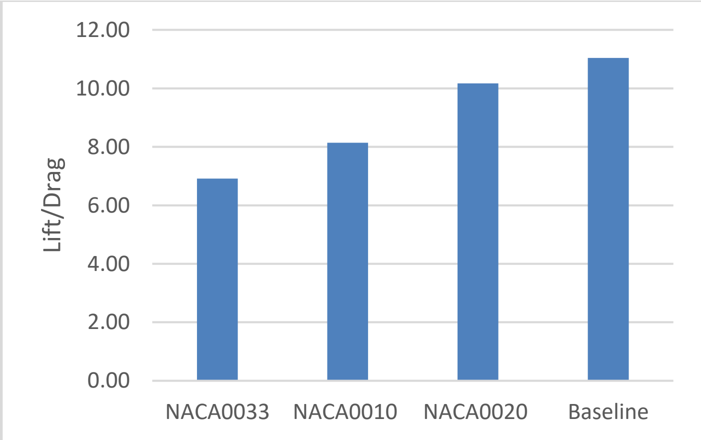

Fig. 13 Comparison of Lift/Drag ratio for all the four gliders

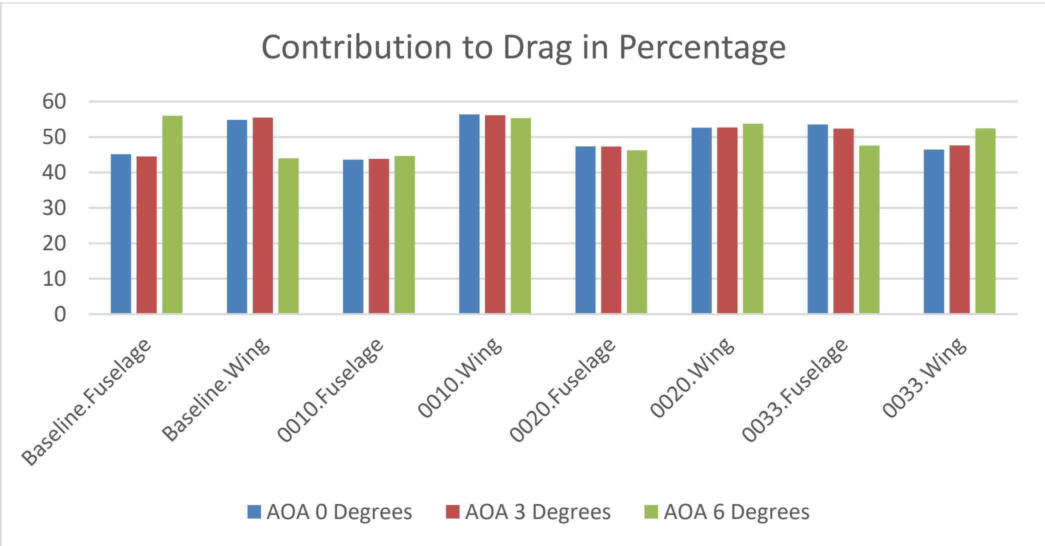

Fig. 14 Contribution of fuselage and wing to the drag of the glider (in percentage)

4. Results

4.1 Comparison of lift and drag forces

The results of the CFD simulations are brought out in this section. For the condition of 0.3 m/s velocities with Angle of attack (α) as 6˚, the drag and lift coefficients (along with their components) of all the four gliders are compared and shown in Figs. 11 and 12 respectively. NACA0033 section exhibits a lower Lift/Drag value and the experimental hull form (based on Myring profile) exhibits the highest L/D value (Fig. 13).

4.2 Comparison of the contribution of fuselage and wing

The comparison of the contribution of the fuselage and wing at various angles of attack was analysed. The same is displayed in Fig. 14 for Drag and Fig. 15 for Lift respectively. The contribution to the net drag decreases with an increase in the angle of attack for the NACA hull forms whereas it increases for the baseline glider.

4.3 Comparison of the mean lift and RMS drag coefficients

The Mean lift Coefficient and Root Mean Square (RMS) Drag Coefficients for all four versions of hull forms estimated by CFD are plotted in Figs. 16 and 17 respectively. Further, the mean Lift/Drag ratio of the gliders is plotted against the angle of attack in Fig. 18. A comparison of the velocity of flow developed against all 4 gliders is shown in Fig. 19. After curve fitting, the trendlines data of all the four gliders are brought out in Table 2. The table indicates the increasing trend of increase in drag at zero Lift (C_{D0}) as we move from NACA 0010 to NACA 0033. The increase for NACA 0020 is about 12.3% and for NACA 0033 it is found to be 31.5 % compared with the baseline glider. The lift coefficient C_L^{α} indicates a reduction of 13% for NACA 0010 and then an increase of 2% for NACA 0033.

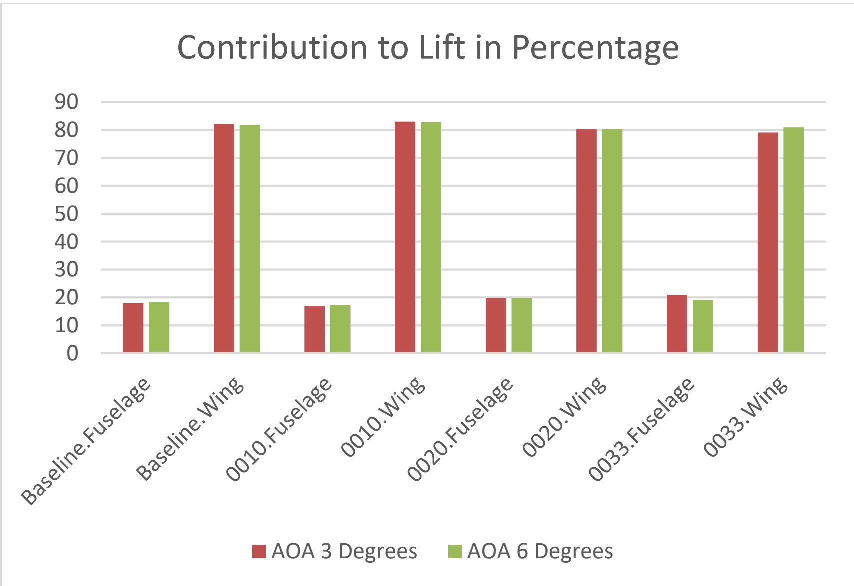

Fig. 15 Contribution of fuselage and wing to the lift of the glider (in percentage)

Table 2 Curve fitting coefficients for Lift and Drag for all the four gliders

Model	C_{DO}	C_D^{α}	C_{L0}	C_L^{α}
Baseline Glider	0.0073	0.0001	0.0004	0.0184
NACA 0010	0.0073	9.00E-05	-7.00E-05	0.0154
NACA 0020	0.0082	0.0001	-0.0003	0.0184
NACA 0033	0.0096	0.0002	-1.00E-05	0.0188

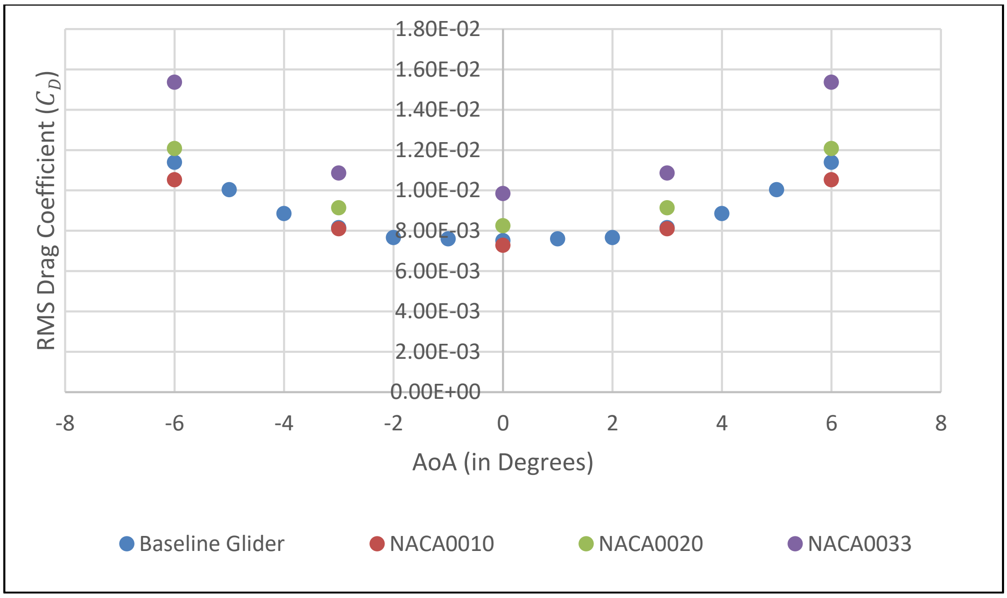

Fig. 16 RMS Drag coefficient vs Angle of attack for all the four gliders

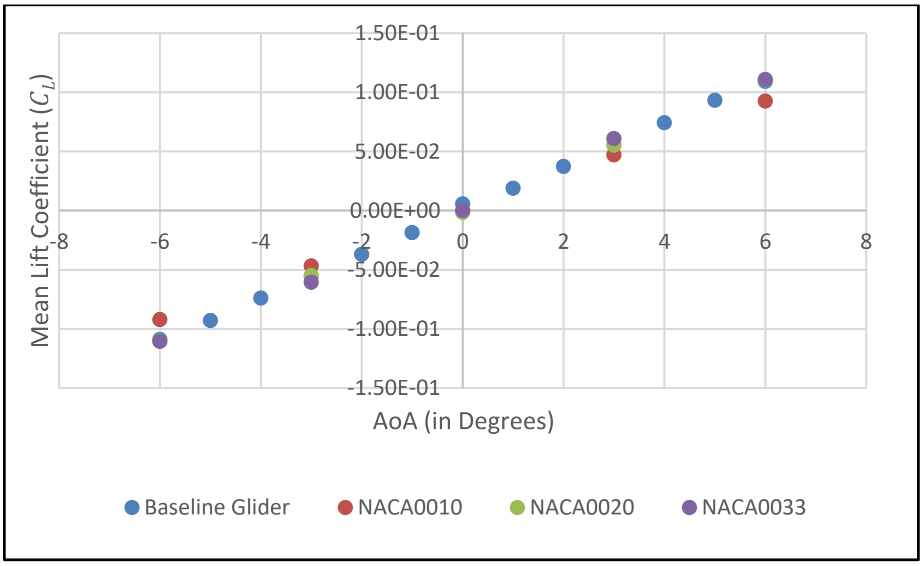

Fig. 17 Mean Lift Coefficient vs Angle of Attack for all four gliders

Table 3 The lowest value of C_P observed at 0.3 m/s and α=0˚

Model	Lowest value of C_P
Baseline Glider	-0.11
NACA 0010	-0.091
NACA 0020	-0.22
NACA 0033	-0.45

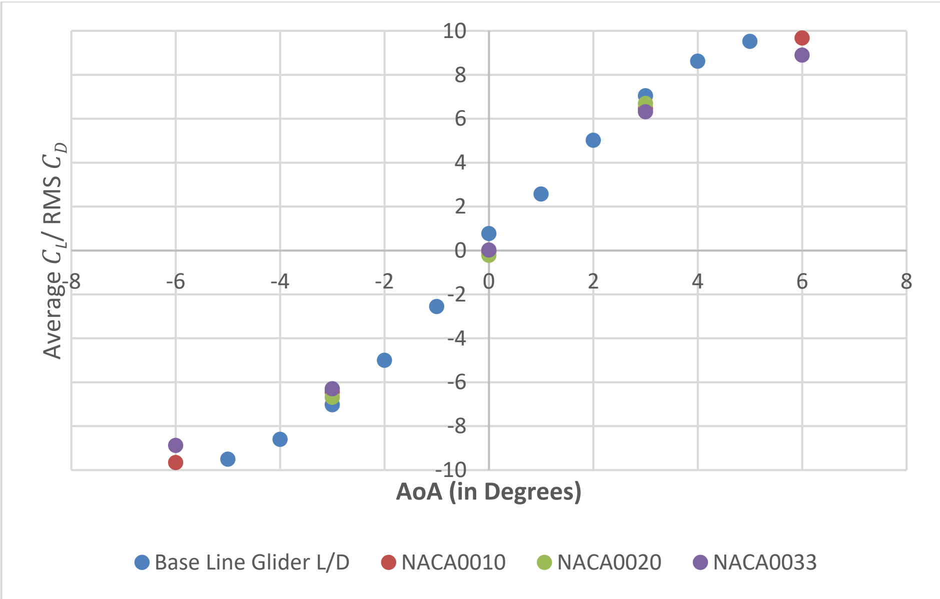

Fig. 18 Mean L/D vs Angle of attack for all four gliders

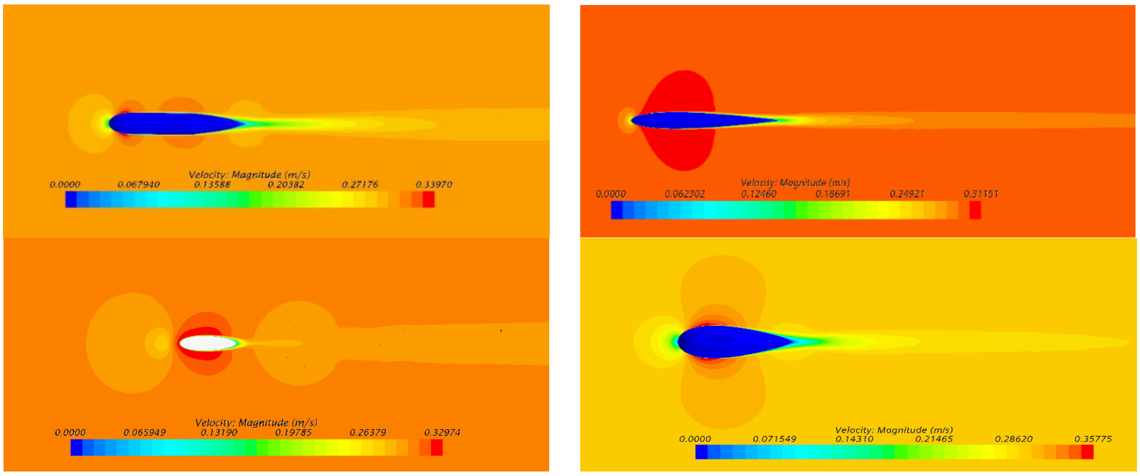

Fig. 19 Velocity scalars for the four gliders at velocity 0.3 m/s and α=0˚

A comparison of the pressure coefficients for the four gliders, across the length of the glider, is shown in Fig. 20. The values of the lowest observed C_P is shown in Table 3.

5. Analysis of the results

The CFD results indicate salient points that are useful for designers choosing hull forms to cover the pressure hull. The same are discussed in the following paragraphs.

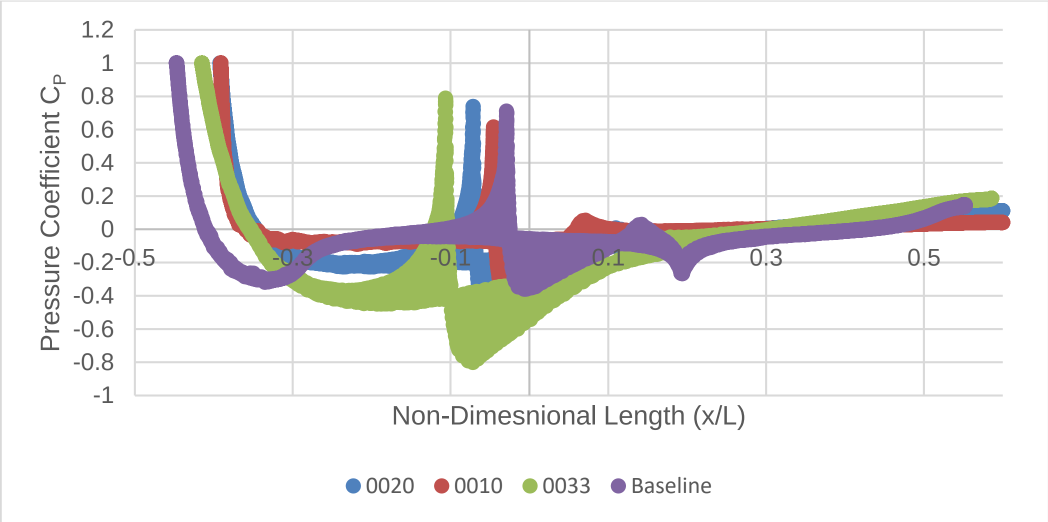

Fig. 20 Velocity contours for the four gliders with the angle of attack 6˚ and at a velocity of 0.3 m/s

Table 4 Estimated Radius of spiral path for the candidate gliders

Model	C_{D0}	% Change in C_{D0} w.r.t candidate glider	Estimated Radius
Baseline Glider	0.0073	-	R
NACA 0010	0.0073	0	R
NACA 0020	0.0082	12.33	0.8767R
NACA 0033	0.0096	31.51	0.6849R

- A legacy shaped underwater glider, whose hull form is shaped out of an ellipsoid, and paraboloid, for a constant volume, will lie between NACA 0010 and NACA 0020 in terms of Length, Span and Lift and Drag characteristics.
- An increase in Drag of the body is noticed for Bodies of Revolutions of NACA sections when moving from 0010 to 0033. This can be inferred from Fig. 13, Fig. 18 and the value of C_{D0} in Table 2.
- NACA0033 section exhibits a lower Lift/Drag value and the experimental hull form exhibits the highest L/D value.
- The Lift characteristics do not display a major variation for the NACA sections. This is obtained from Figs. 14, 19, 20 and C^{α}_{L} values in Table 2.
- A decrease in the overall length of the body is pertinent when moving from NACA0010 to NACA 0033. However for the same volume, and fixed-wing chord, the value of diameter and span of the vehicles do not display large variation.
- As indicated in the Figs. 16 and 17, the frictional drag value for all four gliders decreased with increasing angle of attack (for the same velocity) and the pressure drag value increases with an increase in the angle of attack.

- The contribution to the net drag decreases with an increase in the angle of attack for the NACA hull forms whereas it increases for the baseline glider.
- The flow characteristics across the four glider fuselages are shown in Fig. 21. Since the $\alpha=0^{\circ}$, the velocity across the fuselage is symmetrical along the longitudinal centre line.
- The typical flow features of a stagnation point in the foremost point of the fuselage and the increase and decrease in velocity across the fuselage is same in all the four vehicles. However, the velocity attained at the highest point differ.
- The lowest value of pressure coefficient C_P is observed for the NACA 0033 fuselage and the highest value of C_P is observed for the NACA 0010 fuselage which reflects the higher drag of NACA 0033 and lower drag of NACA 0010 (refer to Figure 22 and Table 3).
- A study by the authors has indicated that for a glider executing a turn initiated by a rudder, the radius of the spiral path is sensitive to the C_{D0} of the glider. Similarly, the longitudinal motion is also dependent on the Lift coefficient and L/D value of the glider (Rayaprolu and Vijayakumar 2021). The designer could hence choose a stubby NACA0033 or NACA0020 over the torpedo shaped hull for a glider that requires to execute the turning motion in a vertical column of the area of interest.
- Based on the sensitivity analysis, the sensitivity of the radius of the spiral path to the HDC C_{D0} is 0.705 (Fig. 5 refers). Here we focus on the sensitivity of radius on the drag coefficient alone as it is found to be the highest amongst the other fuselage/wing coefficients (HDCs dependent on the rudder are neglected as rudder is a control surface).
- Further, an increase in the drag coefficient will lead to decrease in the radius of the spiral path. Hence, the estimated radius for the fuselages, with the radius of the candidate glider for a given rudder angle being "R" and the rudder angle kept constant, is as shown in Table 4.

6. Conclusions

The current study involves CFD analysis of a baseline glider and variants of the same using NACA body of revolution sections as candidate fuselages. The study has been undertaken with the volume of the entire glider kept constant and varying the hull form. The results indicate a significant variation in Drag characteristics of the glider and a lesser change in Lift characteristics. The authors believe that such a study would enable designers to choose mission-specific glider hull forms. The significant drag characteristic can play a key role in the glider trajectory when undertaking a turning maneuver. A comparative study of the HDCs of underwater gliders aids in plugging the gap in the literature. The novelty of the study, the authors opine, lies in the comprehensive study of the Lift, Drag and Pressure behaviour of a vehicle of the same volume and same wings but different fuselage shape.

However, a true parametric study is warranted for understanding the effect of change of hull form on the underwater glider characteristics. This can be undertaken by varying the curvature of the ellipsoid and paraboloid of the entrance and run of a vehicle and studying the effect of change of flow characteristics around the body. This research is in progress by the authors and is intended as future work.

References

Arima, M., Ichihashi, N. and Ikebuchi, T. (2008), "Motion characteristics of an underwater glider with independently controllable main wings", *OCEANS'08 MTS/IEEE Kobe-Techno-Ocean'08 - Voyage toward the Future, OTO'08*, 156-161. https://doi.org/10.1109/OCEANSKOBE.2008.4531062.

Guggilla, M. and Rajagopalan, V. (2019), "Autonomous underwater gliders – A brief review of development and design and a proposed model for virtual mooring", *Proceedings of the International Conference on Coastal and Inland Water Systems 2019*.

Guggilla, M. and Rajagopalan, V. (2020), "CFD investigation on the hydrodynamic characteristics of blended wing unmanned underwater gliders with emphasis on the control surfaces", *Proceedings of the International Conference on Offshore Mechanics and Arctic Engineering - OMAE*, *6*B-*2020*. https://doi.org/10.1115/omae2020-19280.

Guggilla, M. and Rajagopalan, V. (2018), "Study on the Hydrodynamic performance of unmanned underwater glider with varying wing section using CFD", *MARHY 2018*, 1-8. http://www.doe.iitm.ac.in/vijay2028/publications.

Guggilla, M. andVijayakumar, R. (2019a), "CFD study of the hydrodynamic characteristics of blended winged unmanned underwater gliders", *Proceedings of the International Offshore and Polar Engineering Conference*.

Guggilla, M. and Vijayakumar, R. (2019b), "CFD Study of the Hydrodynamic Characteristics of Blended Winged Unmanned Underwater Gliders", *Proceedings of the 29th (2019) International Ocean and Polar Engineering Conference*, 1547-1552. http://www.isope.org/wp-content/uploads/2019/06/Pap-2019-Honolulu-Web-3-0430-MK-jc-test2-space85-use-1touch-0610.pdf.

Harry Jackson, C.A. (1992), "Fundamentals of submarine concept design", *SNAME Transactions*, **100**, 419-448.

Heaslet, M.A. and Nitzberg, G.E. (1947), "The calculation of drag for airfoil sections and bodies of revolution at subcritical speeds", In *NACA Research Memorandum: Vol. RM No. A7B*.

Hockley, C.J. (2018), *Improving Seaglider Efficiency : an Analysis of Wing Shapes, Hull Morphologies , and Propulsion Methods* (Issue July), Embry-Riddle Aeronautical University.

Hoerner, S.F. (1965), "Fluid-dynamic drag", In *Hoerner Fluid Dynamics* (1965th ed.). https://ci.nii.ac.jp/naid/20000254063.

ITTC - Recommended Procedures and Guidelines. (2011), "Practical guidelines for ship CFD", *Proceedings of the 26th International Towing Tank Conference*.

Jagadeesh, P., Murali, K. and Idichandy, V.G. (2016), "Experimental investigation of hydrodynamic force coefficients over AUV hull form", *Ocean Eng.*, **2**(1), 90-119. https://doi.org/10.1016/j.joes.2017.03.003.

Joubert, P.N., Hoffmann, P.H. and Sinclair, T.J. (1978), "Further study of bodies of revolution", *J. Ship Res.*, **22**(1), 54-63. https://doi.org/10.5957/jsr.1978.22.1.54.

Krasnov, N.F. (1971). "Aerodynamics of bodies of revolution", *J. Fluid Mech.*, **50**(2). https://doi.org/10.1017/S0022112071222643.

Li, J., Wang, P., Dong, H., Wu, X., Chen, X.. and Chen, C. (2020), "Shape optimisation of blended-wing-body underwater gliders based on free-form deformation", *Ships Offshore Struct.*, **15**(3), 227-235. https://doi.org/10.1080/17445302.2019.1611989.

Li, X., Zhao, M., Zhao, F., Yuan, Q. and Ge, T. (2014), "Study on hydrodynamic performance of Heavier-than-water AUV with overlapping grid method", *Ocean Syst. Eng.*, **4**(1), 1-19. https://doi.org/10.12989/ose.2014.4.1.001.

Lidtke, A.K., Turnock, S.R. and Downes, J. (2018), "Hydrodynamic design of underwater gliders using k-kL-ω reynolds averaged navier-stokes transition model", *IEEE J. Oceanic Eng.*, **43**(2), 356-368. https://doi.org/10.1109/JOE.2017.2733778.

Lidtke, A.K., Turnock, S.R. and Downes, J. (2016), "Assessment of underwater glider performance through viscous computational fluid dynamics", *Autonomous Underwater Vehicles 2016, AUV 2016*, 364-373. https://doi.org/10.1109/AUV.2016.7778698.

Mises, R. Von. (1945), *Theory of flight* (First), McGraw-Hill Book Company.

Muhammad Yasar, J., Mark, O., Nagarajan, T., Ali, S.S.A. and Barkat, U. (2015), "Study on wing aspect ratio on the performance of a gliding robotic fish", *Appl. Mech. Mater.*, **786**, 248-253. https://doi.org/10.4028/www.scientific.net/amm.786.248.

Ray, A., Singh, S.N. and Seshadri, V. (2011), "Underwater gliders - Force multipliers for naval roles", *RINA, Royal Institution of Naval Architects - Warship 2011: Naval Submarines and UUVS, Papers*, 29-41.

Rayaprolu, V.S.S. and Vijayakumar, R. (2021), "Sensitivity analysis of the turning motion of an underwater glider on the viscous hydrodynamic coefficients", *Defence Sci. J.*, **71**(5), 709-717. https://doi.org/10.14429/dsj.71.16905.

Saunders, A. and Nahon, M. (2002), "The effect of forward vehicle velocity on through-body AUV tunnel thruster performance", *Oceans Conference Record (IEEE)*, **1**(4), 250-259. https://doi.org/10.1109/oceans.2002.1193280.

Shankar, R.V.S. and Vijayakumar, R. (2020). "Numerical study of the effect of wing position on autonomous underwater glider", *Defence Sci. J.*, **70**(2), 214-220. https://doi.org/10.14429/dsj.70.14742

Shashank Shankar, R.V. and Vijayakumar, R. (2019). "Effect of rudder and roll control mechanism on path prediction of autonomous underwater gliders", *Lecture Notes in Civil Engineering*, **22**, 491-506. https://doi.org/10.1007/978-981-13-3119-0_29.

Shashank, R.V. and Vijayakumar, R. (2019), "Maneuverability and dynamics of autonomous underwater gliders : Study and review of the spiral path maneuver", *Trans. R Inst. Nav. Archit. Part B–Int. J. Small Cr.*, **161**(2), 1-15.

Singh, Y., Bhattacharyya, S.K. and Idichandy, V.G. (2017), "CFD approach to modelling, hydrodynamic analysis and motion characteristics of a laboratory underwater glider with experimental results", *J. Ocean Eng. Sci.*, ***2***(2), 90-119. https://doi.org/10.1016/j.joes.2017.03.003.

Stevenson, P., Furlong, M. and Dormer, D. (2007), "AUV shapes - Combining the practical and hydrodynamic considerations", *OCEANS 2007 - Europe*, *070312*, 1-6. https://doi.org/10.1109/oceanse.2007.4302483.

Stryczniewicz, K., Stryczniewicz, W. and Szczepaniak, R. (2019), "Modelling hydrodynamic characteristics of the underwater glider based on computational fluid dynamics", *IOP Conf. Series: Mater. Sci. Eng.*, **710**, 012012. https://doi.org/10.1088/1757-899X/710/1/012012.

Sun, S., Song, B., Wang, P., Dong, H. and Chen, X. (2021), "A new simplified numerical approach for shape design of underwater wings", *Ships Offshore Struct.*, **17**(8), 1-11. https://doi.org/10.1080/17445302.2021.1937804.

Ting, M.C., Abdul Mujeebu, M., Abdullah, M.Z. and Arshad, M.R. (2012), "Numerical study on hydrodynamic performance of shallow underwater glider platform", *Indian J. Marine Sci.*, **41**(2), 124-133.

Wang, Y., Zhang, Y., Zhang, M.M., Yang, Z. and Wu, Z. (2017), "Design and flight performance of hybrid underwater glider with controllable wings", *Int. J. Adv. Robot. Syst.*, **14**(3). https://doi.org/10.1177/1729881417703566.

Zhang, F., Zhang, F. and Tan, X. (2014), "Tail-enabled spiraling maneuver for gliding robotic fish", *J. Dyn. Syst. Measurement Control T. ASME*, **136**(4), 041028. https://doi.org/10.1115/1.4026965.

Zhang, S., Yu, J., Zhang, A.. and Zhang, F. (2013), "Spiraling motion of underwater gliders: Modeling, analysis, and experimental results", *Ocean Eng.*, **60**, 1-13. https://doi.org/10.1016/j.oceaneng.2012.12.023.

RS